2023 IEEE 9th International Workshop on Computational Advances in Multi-Sensor Adaptive Processing (CAMSAP) | 979-8-3503-4452-3/23/$31.00 ©2023 IEEE | DOI: 10.1109/CAMSAP58249.2023.10403442

Parameterized Inverse Eigenvalue Problem for Quantum Sensing

Kyle Wright
Department of Applied Mathematics
University of California, Merced
Merced, CA
kwright11@ucmerced.edu

Roummel Marcia
Department of Applied Mathematics
University of California, Merced
Merced, CA
rmarcia@ucmerced.edu

Michael Scheibner
Department of Physics
University of California, Merced
Merced, CA
mscheibner@ucmerced.edu

Boaz Ilan
Department of Applied Mathematics
University of California, Merced
Merced, CA
bilan@ucmerced.edu

***Abstract*—A system of tunnel-coupled quantum dots is considered in the presence of an applied electric field. Given the measurements of differences between ground state and excited state energy levels as the electric field is varied, we seek to recover the quantum Hamiltonians that describe this system. We formulate this as a parameterized inverse eigenvalue problem and develop algebraic and computational methods for solving for parameters to represent these Hamiltonians. The results demonstrate that this approach is highly precise even when there is error present within the measurements. This theory could aid in the design of high resolution tunable quantum sensors.**

***Index Terms*—Quantum sensing, inverse eigenvalue problems, Gröbner basis, optimization**

I. Introduction

The control of photonic transport in nonequilibrium quantum systems has recently garnered much interest. Our research is motivated by the emerging field of quantum metrology, which opens the door for high-resolution sensing of gravitation, acoustic waves, electric, magnetic and other fields [1]–[10]. For simplicity, we consider a system of two quantum dots (QDs), which contains a positive trion, *i.e.*, one electron and two holes, and which is subject to an applied electric field. The effective dynamics can be described by a quantum master equation, whose steady-state possesses discrete energy levels. The general problem is to recover the intrinsic physical parameters, such as spin-coupling strength, from measurements of differences between energy levels as the applied electric field is varied. This can be formulated as an inverse eigenvalue problem (IEP), which depends on a "tunable" parameter (the applied electric field). We develop efficient mathematical and computational methods for solving such problems accurately.

II. Problem Description

The steady-state energy levels of the two coupled QDs correspond to eigenvalues of quantum Hamiltonians. Specifically, we assume that the ground state and first excited state are described by 2×2 and 3×3 symmetric matrices, respectively [11]. The diagonal elements of these matrices depend on the applied electric field strength, F. The off-diagonal elements are independent of F, which is a good approximation for weak electric fields or weak tunnel coupling. The ground state matrix has the form

$$G(F) = \begin{bmatrix} y_1 & y_0 \\ y_0 & \alpha_0 + \beta_0 F \end{bmatrix}, \tag{1}$$

where y_0, y_1 and α_0, β_0 are all real-valued (y_1 could depend linearly on F as well, but this would not matter as discussed below). The excited state matrix has the form

$$H(F) = \begin{bmatrix} h_1(F) & x_0 & x_0 \\ x_0 & h_2(F) & 0 \\ x_0 & 0 & h_3(F) \end{bmatrix}, \tag{2}$$

where $h_1(F), h_2(F)$, and $h_3(F)$ are quadratic in F, *i.e.*,

$$h_i(F) = \alpha_i + \beta_i F + \gamma_i F^2, \quad i = 1, 2, 3\ , \tag{3}$$

with real coefficients. For simplicity, we have assumed that the $(1,2)$ and $(1,3)$ elements of $H(F)$ are equal and that the $(2,3)$ and $(3,2)$ elements are zero. However, the methods described below can be applied even when these assumptions are relaxed. Consistent with experimental results, we also make the following assumptions. The off-diagonal elements are positive, *i.e.*, $y_0 > 0, x_0 > 0$. The linear coefficients satisfy: $\beta_0 < 0$ and $|\beta_1| \ll |\beta_{2,3}|$, $\beta_2 \approx \beta_3$. The quadratic terms are much smaller than the other terms. In addition, x_0 is small. The electric field is in a range $F_{\min} \le F \le F_{\max}$, such that for all F in this range: $h_2(F) > h_3(F)$. These conditions guarantee real, distinct eigenvalues.

The physical measurements correspond to the *differences* between the eigenvalues of G and H. Our objective is to recover the parameters that define G and H from these differences. To this end, we denote the eigenvalues of

This research is partially supported by NSF grants DMS 1840265 and DMS 2125510.

$G(F)$ by $\{\xi_1(F), \xi_2(F)\}$ and the eigenvalues of $H(F)$ by $\{\lambda_1(F), \lambda_2(F), \lambda_3(F)\}$. Let $C_{i,j}(F)$ be the difference between the i^{th} eigenvalue of $H(F)$ and the j^{th} eigenvalue of $G(F)$, *i.e.*,

$$C_{i,j}(F) = \lambda_i(F) - \xi_j(F), \quad i = 1, 2, 3, \quad j = 1, 2\ . \tag{4}$$

For an illustration, see Fig. 1. The X-pattern that appears in this figure is a common feature in the experimental data [8], [11]–[13]. The examples provided below correspond to what is experimentally observed in spectroscopic measurements of InAs/GaAs coupled dots. The ability to recover accurately the coefficients that define G and H is of practical interest, especially if the number of input measurements needed to do so is not large. For example, this could help to drastically reduce the time needed to catalog suitable coupled QD pairs in a sample that contains $O(10^8)$ dot pairs per cm^2 or more. Likewise, this could be employed to identify variations in the measurement response due to an external stimulus, such as an electric, magnetic, or other field, and hence assist in sensing applications.

Consider any scalar multiple of the identity matrix that is linear in F as $L(F) = (\delta + \eta F)I$ with constants $\delta, \eta \in \mathbb{R}$. It follows that adding $L(F)$ to both $G(F)$ and $H(F)$ would shift each of the eigenvalues by $(\delta + \eta F)$, thus yielding the same $C_{i,j}(F)$. Hence, the diagonals of G and H can only be determined up to an additive linear function of F. This also explains why y_1 was chosen to be constant. Moreover, owing to this invariance, without loss of generality, we assume that $y_1 = 0$ in (1).

To recap, given the measurements $C_{i,j}(F)$ (defined in (4)) for a set of electric field values $\{F_1, F_2, \ldots, F_n\}$, we seek to recover the coefficients that define $G(F)$ and $H(F)$, namely the vectors of parameters

$$\vec{p}_G = [y_0, \alpha_0, \beta_0] \in \mathbb{R}^3 \text{ and } \vec{p}_H = [x_0, \vec{p}_{h_1}, \vec{p}_{h_2}, \vec{p}_{h_3}] \in \mathbb{R}^{10}\ , \tag{5}$$

where $\vec{p}_{h_i} = [\alpha_i, \beta_i, \gamma_i] \in \mathbb{R}^3$ for $i = 1, 2, 3$.

Related work: Broadly speaking, inverse eigenvalue problems involve reconstructing a matrix with specified spectral information. These problems are structured and are motivated from a variety of applications in signal processing, physics, chemistry, and engineering. For a general overview of such applications, how they give rise to IEPs and their theory, see [14]–[17]. There are generally three types of IEPs: parameterized [18], structured [19], and partially described [20], [21]. Much of the literature on parameterized IEPs (PIEPs) focuses on linear PIEPs. Our work differs from existing work in two main ways: (i) the measured data corresponds to the *differences* between eigenvalues of two separate matrices and (ii) the parameterization of the matrices' elements depends on the applied electric field *nonlinearly*.

III. Proposed Approach

In this section we recover the coefficients $\vec{p}_G$ in $G(F)$ and obtain an algebraic formulation for recovering the coefficients $\vec{p}_H$ in $H(F)$.

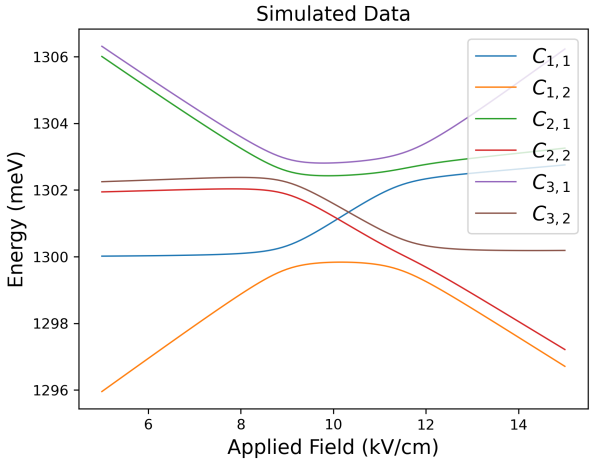

Fig. 1. Simulated eigenvalue differences, $C_{i,j}(F) = \lambda_i(F) - \xi_j(F)$ with $i = 1, 2, 3$ and $j = 1, 2$.

A. Recovering the coefficients in $G(F)$

The eigenvalues of $G(F)$ are given explicitly by

$$\xi_{1,2}(F) = \frac{1}{2}(\alpha_0 + \beta_0 F) \ \pm \ \sqrt{(\alpha_0 + \beta_0 F)^2 + 4y_0^2}. \tag{6}$$

From (4) we get that $C_{i,2} - C_{i,1} = \xi_2 - \xi_1$ for all F and i. It follows from (4) and (6) that

$$[C_{i,2}(F) - C_{i,1}(F)]^2 = \beta_0^2 F^2 + 2\alpha_0\beta_0 F + \alpha_0^2 + 4y_0^2. \tag{7}$$

Assuming that the set $\{C_{i,j}(F)\}$ is known for (at least) three values of F, we can recover β_0, α_0, and y_0 by solving the least-squares problem

$$\min_{\kappa_0,\kappa_1,\kappa_2} \sum_{k=1}^{n} \sum_{i=1}^{3} \left\{ [C_{i,2}(F_k) - C_{i,1}(F_k)]^2 - (\kappa_2 F_k^2 + \kappa_1 F_k + \kappa_0) \right\}^2 \tag{8}$$

and letting

$$\beta_0 = -\sqrt{\kappa_2}, \ \alpha_0 = \frac{\kappa_1}{2\beta_0}, \ \text{ and } \ y_0 = \frac{1}{2}\sqrt{\kappa_0 - \alpha_0^2}. \tag{9}$$

In our approach, we solve the normal equations associated with (8) to obtain κ_0, κ_1, and κ_2.

B. Algebraic formulation for recovering $H(F)$

Having recovered the coefficients in $G(F)$ using (9), its eigenvalues can be computed readily for *any* F. Hence, the eigenvalues of $H(F)$ can be found for any F from (4), *i.e.*,

$$\lambda_i(F) = C_{i,j}(F) + \xi_j(F), \quad i = 1, 2, 3, \quad j = 1, 2\ . \tag{10}$$

It remains to solve the IEP for $H(F)$ given $\lambda_i(F)$ for a set of F values.

Algebraic formulation. The eigenvalues of $H(F)$ are roots of the characteristic polynomial

$$\det(H(F) - \lambda I) = \zeta_0(\vec{p}_H) + \zeta_1(\vec{p}_H)\lambda + \zeta_2(\vec{p}_H)\lambda^2 - \lambda^3, \tag{11}$$

where, suppressing the dependence on F,

$$\zeta_0(\vec{p}_H) = h_1h_2h_3 - x_0^2(h_2+h_3)\ , \tag{12a}$$
$$\zeta_1(\vec{p}_H) = -(h_1h_2 + h_1h_3 + h_2h_3 - 2x_0^2)\ , \tag{12b}$$
$$\zeta_2(\vec{p}_H) = h_1 + h_2 + h_3\ . \tag{12c}$$

Since the eigenvalues of $H(F)$, λ_1, λ_2, and λ_3, are kno the characteristic polynomial is also given by

$$\det(H(F) - \lambda I) = (\lambda_1-\lambda)(\lambda_2-\lambda)(\lambda_3-\lambda). \quad ($$

Comparing the coefficients in (11) with those in (13) leads the following functions:

$$\tilde{\mathscr{F}}_0(\vec{p}_H) = \zeta_0(\vec{p}_H) - \lambda_1\lambda_2\lambda_3\ , \quad (1$$
$$\tilde{\mathscr{F}}_1(\vec{p}_H) = \zeta_1(\vec{p}_H) + (\lambda_1\lambda_2 + \lambda_1\lambda_3 + \lambda_2\lambda_3)\ , \quad (1$$
$$\tilde{\mathscr{F}}_2(\vec{p}_H) = \zeta_2(\vec{p}_H) - (\lambda_1 + \lambda_2 + \lambda_3)\ , \quad (1$$

whose root defines the desired parameters in $H(F)$. S tem (14) can be decoupled using the Gröbner basis of t system relative to $\{h_i\}_{i=1}^3$ (which can be obtained usin process akin to Gaussian elimination for linear systems):

$$\begin{aligned}\mathscr{F}_0(x_0,\vec{p}_{h_1}) &= \tilde{\mathscr{F}}_0(\vec{p}_H) + h_1\tilde{\mathscr{F}}_1(\vec{p}_H) + (h_1^2+x_0^2)\tilde{\mathscr{F}}_2(\vec{p}_H)\\ &= 3h_1x_0^2 + h_1^3 + h_1(\lambda_1\lambda_2+\lambda_1\lambda_3+\lambda_2\lambda_3)\\ &\quad - (h_1^2+x_0^2)(\lambda_1+\lambda_2+\lambda_3) - \lambda_1\lambda_2\lambda_3,\end{aligned} \tag{15a}$$

$$\begin{aligned}\mathscr{F}_1(\vec{p}_{h_2}) &= \tilde{\mathscr{F}}_1(\vec{p}_H) + (h_1+h_2)\tilde{\mathscr{F}}_2(\vec{p}_H)\\ &= h_1^2 + h_2h_1 + h_2^2 + 2x_0^2 + \lambda_1\lambda_2 + \lambda_1\lambda_3\\ &\quad + \lambda_2\lambda_3 + (h_1+h_2)(\lambda_1+\lambda_2+\lambda_3),\end{aligned} \tag{15b}$$

$$\mathscr{F}_2(\vec{p}_{h_3}) = \tilde{\mathscr{F}}_2(\vec{p}_H). \tag{15c}$$

In contrast to the functions in (14), whose roots must be determined simultaneously, the functions in (15) can determine the roots *sequentially*. Specifically, the parameters x_0 and $\vec{p}_{h_1}$ are obtained first using (15a), as described below. Having obtained $\vec{p}_{h_1}$, the parameters $\vec{p}_{h_2}$ can be obtained using (15b). Finally, $\vec{p}_{h_3}$ can be readily obtained from (15c).

C. Computational method

To find the roots of the functions in (15), we solve equivalent optimization problems whose minima correspond to the roots of the $\mathscr{F}_i$'s. First, we solve

$$\underset{x_0,\vec{p}_{h_1}}{\text{minimize}} \quad \sum_{k=1}^{n}\left[\mathscr{F}_0(x_0,\vec{p}_{h_1},F_k)\right]^2. \tag{16}$$

In the absence of measurement errors, any four values of F, *i.e.*, $n = 4$, are both necessary and sufficient for solving (15a) to obtain x_0 and $\vec{p}_{h_1}$. Those same values of F can then be used for solving (15b) and (15c) for $\vec{p}_{h_2}$ and $\vec{p}_{h_3}$ by solving minimization problems similar to (16). We shifted the eigenvalues by subtracting their mean. This improves the estimation of the coefficients by reducing the magnitude differences among the coefficients.

In our numerical experiments, we use five equally spaced values of F and solve (16) and those corresponding to $\mathscr{F}_1$ and $\mathscr{F}_2$ using a trust-region approach [22], which solves a sequence of constrained subproblems that use quadratic approximations of the objective function. We used the *"trust-exact"* method in Python's *scipy.optimize.minimize* package. Similar results were also obtained using line-search methods.

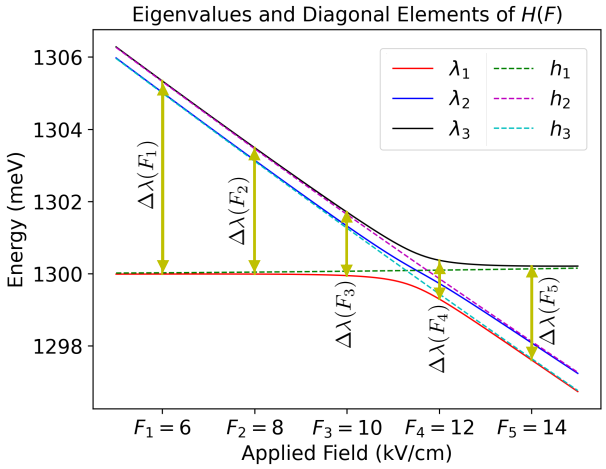

Fig. 2. Simulated eigenvalues (λ_1, λ_2, and λ_3) and diagonal elements (h_1, h_2, and h_3) of $H(F)$. Here, $\Delta\lambda(F_k)$ is defined as in (18).

D. Initialization

Here we propose a protocol for obtaining a good initial iterate for the coefficients. To illustrate this we refer to the example provided by Fig. 2, where five measurements occur at five equi-spaced F values denoted by the tick marks. For each F, the values of λ_i $(i=1,2,3)$ are obtained as described above. To estimate the parameter vector $\vec{p}_{h_1}$, we note that in Fig. 2, we have $h_1(F_1) \approx \lambda_1(F_1)$, $h_1(F_2) \approx \lambda_1(F_2)$, and $h_1(F_5) \approx \lambda_3(F_5)$. To compute an approximation to $\vec{p}_{h_1} = [\alpha_1, \beta_1, \gamma_1]$, we then solve the least-squares solution to

$$\alpha_1 + \beta_1F_1 + \gamma_1F_1^2 = \lambda_1(F_1), \tag{17a}$$
$$\alpha_1 + \beta_1F_2 + \gamma_1F_2^2 = \lambda_1(F_2), \tag{17b}$$
$$\alpha_1 + \beta_1F_5 + \gamma_1F_5^2 = \lambda_3(F_5). \tag{17c}$$

A similar strategy can be used to obtain estimates for $\vec{p}_{h_2}$ and $\vec{p}_{h_3}$. To determine which F values and which eigenvalues to use in the least-squares problem, we consider the differences between the extremal eigenvalues,

$$\Delta\lambda(F_k) = |\lambda_3(F_k) - \lambda_1(F_k)|, \quad k = 1,\ldots,5\ . \tag{18}$$

In Fig. 2, they are ordered as $\Delta\lambda(F_4) < \Delta\lambda(F_3) < \Delta\lambda(F_5) < \Delta\lambda(F_2) < \Delta\lambda(F_1)$. We choose those 3 values of F_k that have the largest $\Delta\lambda(F_k)$, *i.e.*, $k = 1, 2, 5$, which provide the best values of F to approximate $h_1(F)$. The initial iterate for x_0 can be easily obtained from (14b) at $F = F_4$. To most accurately estimate x_0, it is best to use a value of F where the diagonal elements are least similar to the eigenvalues, which occurs at $F = F_4$ in this case. Overall, we find that this protocol yields good initial iterates, using which the optimization method converges robustly to an accurate solution.

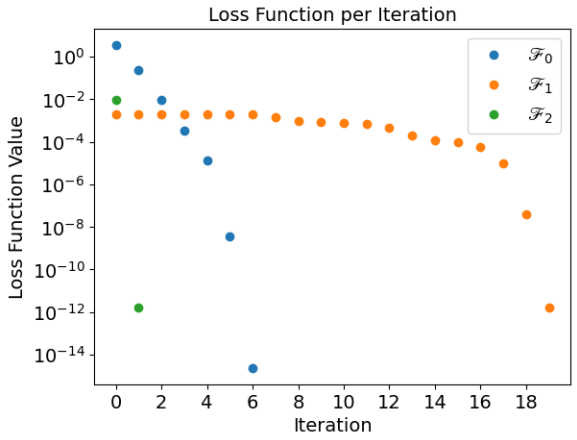

Fig. 3. Values of loss functions using $\mathscr{F}_0$, $\mathscr{F}_1$, $\mathscr{F}_2$ as functions of iterations using a trust-region approach with no noise in the data.

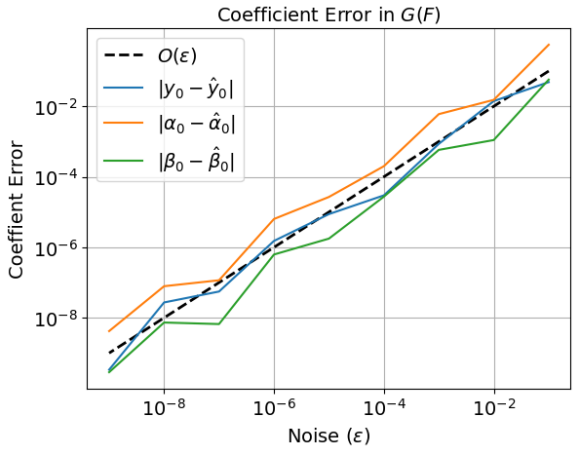

Fig. 4. Error in the coefficient vector $\vec{p}_G$ as a function of noise in the data.

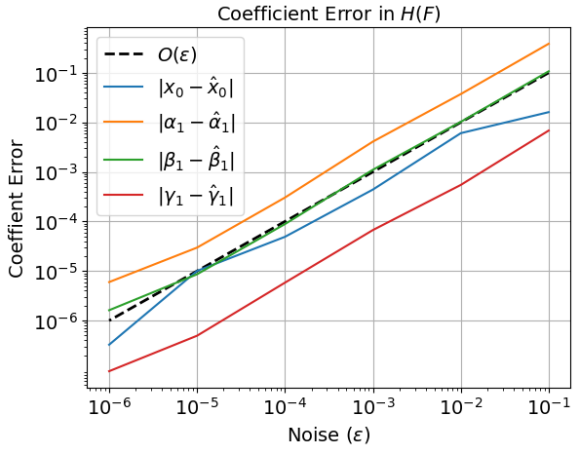

Fig. 5. Error in the coefficient vector $\vec{p}_{h_1}$ as a function of noise in the data.

E. Noisy measurements

Noise in the measurements is expected when obtaining the observed eigenvalue differences, $\{C_{i,j}\}$. To measure the impact of noise on the proposed approach, we introduce perturbation, $\tau_i\epsilon$, at each $C_{i,j}$, where $\tau_i \in \{-1, 1\}$ is a binary random variable and $\epsilon \in \mathbb{R}$:

$$\tilde{C}_{i,j} = C_{i,j} + (-1)^{\tau_i}\epsilon \tag{19}$$

We found that using the approach in Sec. III-D consistently generated an initial iterate that led to the minimizer of (16).

IV. Numerical Results

We conducted numerical experiments to test the efficacy of the proposed approach outlined in Sec. III using both noiseless and noisy measurements. For the results shown in this section, we used simulated measurement values from Fig. 1. These values were created with $\vec{p}_G = [0.35, 9, -1]$, $x_0 = 0.3$, $\vec{p}_{h_1} = [1300.0, -4.0 \times 10^{-4}, 7.0 \times 10^{-4}]$, $\vec{p}_{h_2} = [1311.14, -1.0, 0.005]$, and $\vec{p}_{h_3} = [1310.86, -1.0, 0.004]$ at F values 6, 8, 10, 12, and 14.

Experiment I: Noiseless measurements. Using noiseless measurements, we achieved machine precision in estimating $\vec{p}_G$ and $\vec{p}_H$. When recovering the coefficients in $\vec{p}_H$, we observed the loss functions created in (16) converge to zero as the iterations increased, as shown in Fig. 3. This shows that our proposed approach is appropriate to use when recovering the coefficients in $\vec{p}_G$ and $\vec{p}_H$.

Experiment II: Noisy measurements. To determine the effects of noise on our proposed approach, we simulated noise in the measurements of eigenvalue differences using (19) for different values of ϵ. We then implemented our proposed method using these noisy measurements and observed the error in the coefficients of $\vec{p}_G$ and $\vec{p}_H$ for these values of ϵ. In Fig. 4 we observe an $O(\epsilon)$ relationship between the coefficients in $\vec{p}_G$ and ϵ. We observed a similar relationship between ϵ and the coefficients in $\vec{p}_H$. The coefficient error versus ϵ for x_0 and $\vec{p}_{h_1}$ can be observed in Fig. 5, and similar patterns can also be observed for $\vec{p}_{h_2}$ and $\vec{p}_{h_3}$. This shows that the proposed method is both robust in the presence of noise and produces a predictable decrease in coefficient error as noise is reduced.

V. Conclusions

The method proposed in this paper successfully recovers ground and excited state coefficients using measurements simulating observed eigenvalue differences from our motivating example. We have demonstrated that, under some assumptions, the ground state coefficients can be recovered and used to reduce the problem to a parameterized IEP. Our proposed method is able successfully solve the parameterized IEP using a series of systems of equations to recover the excited state coefficients. Through the use of a good initial iterate using asymptotic relationships and instead solving a related parameterized IEP, the proposed method is also robust to noise in the measurements. This method can be adapted for use in solving similar problems with various applications in quantum sensing.

REFERENCES

[1] S. Pirandola, B. R. Bardhan, T. Gehring, C. Weedbrook, and S. Lloyd, "Advances in photonic quantum sensing," *Nature Photonics*, vol. 12, no. 12, pp. 724–733, 2018.

[2] S. Walborn, A. Pimentel, L. Davidovich, and R. de Matos Filho, "Quantum-enhanced sensing from hyperentanglement," *Physical Review A*, vol. 97, no. 1, p. 010301, 2018.

[3] B. Stray, A. Lamb, A. Kaushik, J. Vovrosh, A. Rodgers, J. Winch, F. Hayati, D. Boddice, A. Stabrawa, A. Niggebaum *et al.*, "Quantum sensing for gravity cartography," *Nature*, vol. 602, no. 7898, pp. 590–594, 2022.

[4] K. J. Satzinger, Y. Zhong, H.-S. Chang, G. A. Peairs, A. Bienfait, M.-H. Chou, A. Cleland, C. R. Conner, É. Dumur, J. Grebel *et al.*, "Quantum control of surface acoustic-wave phonons," *Nature*, vol. 563, no. 7733, pp. 661–665, 2018.

[5] C.-Y. Lai, M. Di Ventra, M. Scheibner, and C.-C. Chien, "Tunable current circulation in triangular quantum-dot metastructures," *Europhysics Letters*, vol. 123, no. 4, p. 47002, 2018.

[6] P. Dugar, M. Scheibner, and C.-C. Chien, "Geometry-based circulation of local photonic transport in a triangular metastructure," *Physical Review A*, vol. 102, no. 2, p. 023704, 2020.

[7] C. Jennings, X. Ma, T. Wickramasinghe, M. Doty, M. Scheibner, E. Stinaff, and M. Ware, "Self-assembled inas/gaas coupled quantum dots for photonic quantum technologies," *Advanced Quantum Technologies*, vol. 3, no. 2, p. 1900085, 2020.

[8] M. Scheibner, A. S. Bracker, D. Kim, and D. Gammon, "Essential concepts in the optical properties of quantum dot molecules," *Solid State Communications*, vol. 149, no. 35-36, pp. 1427–1435, 2009.

[9] A. Vamivakas, Y. Zhao, S. Fält, A. Badolato, J. Taylor, and M. Atatüre, "Nanoscale optical electrometer," *Physical Review Letters*, vol. 107, no. 16, p. 166802, 2011.

[10] S. Ramanathan, G. Petersen, K. Wijesundara, R. Thota, E. A. Stinaff, M. L. Kerfoot, M. Scheibner, A. S. Bracker, and D. Gammon, "Quantum-confined stark effects in coupled inas/gaas quantum dots," *Applied Physics Letters*, vol. 102, no. 21, 2013.

[11] M. Scheibner, M. Doty, I. V. Ponomarev, A. S. Bracker, E. A. Stinaff, V. Korenev, T. Reinecke, and D. Gammon, "Spin fine structure of optically excited quantum dot molecules," *Physical Review B*, vol. 75, no. 24, p. 245318, 2007.

[12] E. A. Stinaff, M. Scheibner, A. S. Bracker, I. V. Ponomarev, V. L. Korenev, M. E. Ware, M. F. Doty, T. L. Reinecke, and D. Gammon, "Optical signatures of coupled quantum dots," *Science*, vol. 311, no. 5761, pp. 636–639, 2006.

[13] J. Schall, M. Deconinck, N. Bart, M. Florian, M. von Helversen, C. Dangel, R. Schmidt, L. Bremer, F. Bopp, I. Hüllen, C. Gies, D. Reuter, A. D. Wieck, S. Rodt, J. J. Finley, F. Jahnke, A. Ludwig, and S. Reitzenstein, "Bright electrically controllable quantum-dot-molecule devices fabricated by in situ electron-beam lithography," *Advanced Quantum Technologies*, vol. 4, no. 6, p. 2100002, 2021.

[14] M. T. Chu, "Inverse eigenvalue problems," *SIAM Review*, vol. 40, no. 1, pp. 1–39, 1998.

[15] M. Chu and G. Golub, *Inverse Eigenvalue Problems: Theory, Algorithms, and Applications*. OUP Oxford, 2005.

[16] G. Gladwell, *Inverse Problems in Vibration*. Springer Netherlands, 2005, vol. 10.

[17] A. Kirsch *et al.*, *An Introduction to the Mathematical Theory of Inverse Problems*. Springer, 2011, vol. 120.

[18] H. Dai, Z.-Z. Bai, and Y. Wei, "On the solvability condition and numerical algorithm for the parameterized generalized inverse eigenvalue problem," *SIAM Journal on Matrix Analysis and Applications*, vol. 36, no. 2, pp. 707–726, 2015.

[19] M. T. Chu and G. H. Golub, "Structured inverse eigenvalue problems," *Acta Numerica*, vol. 11, pp. 1–71, 2002.

[20] S.-L. J. Hu and H. Li, "A systematic linear space approach to solving partially described inverse eigenvalue problems," *Inverse Problems*, vol. 24, no. 3, p. 035014, apr 2008.

[21] Z.-J. Bai, S. Serra-Capizzano, and Z. Zhao, "Nonnegative inverse eigenvalue problems with partial eigendata," *Numerische Mathematik*, vol. 120, no. 3, pp. 387–431, 2012.

[22] A. R. Conn, N. I. Gould, and P. L. Toint, *Trust-Region Methods*. SIAM, 2000.